ELSEVIER

Journal of Chromatography A, 828 (1998) 345–356

JOURNAL OF CHROMATOGRAPHY A

Frontal chromatography of proteins: The effect on column performance of the restricted diffusion of molecules in porous chromatographic adsorbents

A.I. Liapis*, H. Sadikoglu, O.K. Crosser

Department of Chemical Engineering and Biochemical Processing Institute, University of Missouri-Rolla, Rolla, MO 65409-1230, USA

Abstract

A theoretical formulation is presented that can be used to describe the dynamic behavior of frontal chromatography of proteins in columns packed with adsorbent particles in which restricted pore diffusion of the adsorbate molecules occurs. The results of this work clearly indicate that the time for breakthrough and the effective utilization of the adsorptive capacity of the chromatographic particles increase as (a) the size of the adsorbate and/or ligand (active site) molecule decreases, (b) the pore connectivity, n_T, of the porous network of the adsorbent particles increases, and (c) the column length, L, increases.

Keywords: Frontal chromatography; Restricted pore diffusion; Adsorbents; Proteins

1. Introduction

A major goal in the study of systems involving the diffusion and adsorption of adsorbate A in porous chromatographic particles, is to determine the dependence of the macroscopic effective pore diffusion coefficient, D_A, of absorbate A on (i) the microscopic (pore) structure of the adsorbent medium (ii) the molecular size of the adsorbate and ligand (active site), and (iii) the fractional saturation of adsorption sites (ligands). Petropoulos et al. [1] constructed and solved a restricted diffusion model which was utilized to simulate the permeability of adsorbate molecules in porous adsorbent particles. Petropoulos et al. [1] considered in their restricted diffusion model the combined effects of steric hindrance at the entrance to the pores and frictional resistance within the pores, as well as the effects of pore size distribution, pore connectivity of the adsorbent, molecular size of adsorbate and ligand (active site), and the fractional saturation of the active sites. The permeability of the adsorbate in porous networks of connectivity n_T was studied by Petropoulos et al. [1] through the use of effective medium approximation (EMA) numerical solutions. The macroscopic effective pore diffusion coefficient, D_A, of adsorbate A in a porous adsorbent particle can be determined from the macroscopic permeability, P_A, of adsorbate A in the porous adsorbent particle by employing equations 25 and 32 presented in the work of Petropoulos et al. [1].

In this work, the effect on column performance of the restricted diffusion of molecules in porous chromatography adsorbents is studied, for column systems involving frontal chromatography of large adsorbate molecules (proteins).

*Corresponding author.

0021-9673/98/$ – see front matter
PII: S0021-9673(98)00642-6

2. Theoretical formulation

In this work, the dynamic adsorption mechanism is considered to be described by the following second-order reversible interaction (McCoy and Liapis [2]):

$$\frac{\partial C_s}{\partial t} = k_1 C_p (C_T - C_s) - k_2 C_s \tag{1}$$

If $\theta (\theta = C_s / C_T)$ is taken to represent the fractional saturation of the active sites, then Eq. (1) takes the following form in terms of the variable θ:

$$\frac{\partial \theta}{\partial t} = k_1 C_p (1 - \theta) - k_2 \theta \tag{2}$$

It is worth noting at this point that at equilibrium $(\partial C_s / \partial t = \partial \theta / \partial t = 0)$ Eqs. (1) and (2) provide the functional form of the Langmuir isotherm. At equilibrium, Eq. (1) becomes

$$C_s = \frac{K C_T C_p}{1 + K C_p} \tag{1a}$$

while Eq. (2) takes the following form:

$$\theta = \frac{K C_p}{1 + K C_p} \tag{2a}$$

In Eqs. (1), (1a), (2), and (2a), the variable C_p represents the concentration of adsorbate A in the pore fluid, C_s denotes the concentration of adsorbate A in the adsorbed phase, C_T represents the maximum concentration of adsorbate A in the adsorbed phase, k_1 and k_2 are the rate constants of the adsorption and desorption steps, respectively, and K $(K = k_1 / k_2)$ is the equilibrium constant.

By employing Eqs. (2) or Eq. (2a) presented above and equations 19 and 32 in Petropoulos et al. [1], the macroscopic permeability, P_A, of adsorbate A can be determined in the porous adsorbent particles for $0 \le \theta \le 1$, when the pore size distribution and pore connectivity of the porous particles are known [1]. The relative permeability, $P_R(\theta)$, of adsorbate A in the porous adsorbent particle is given [1] by

$$P_R(\theta) = \frac{P_A(\theta)}{P_A(\theta = 0)} \tag{3}$$

where $P_A(\theta)$ represents the macroscopic permeability of adsorbate A in the porous adsorbent particles when the fractional saturation of the active sites (ligands) is θ. Equation (25) in Petropoulos et al. [1] relates the macroscopic permeability, P_A, with the macroscopic effective pore diffusion coefficient, D_A, of adsorbate A in the porous adsorbent particles, through the expression

$$D_A = \frac{P_A}{\varepsilon_p} \tag{4}$$

where ε_p represents the porosity of the particle. It should be noted here that both P_A and ε_p vary with θ, and therefore, the macroscopic effective pore diffusion coefficient, D_A, also varies with θ. In Fig. 1, the relative permeability, P_R, versus the fractional saturation of active sites, θ, is presented for a porous adsorbent medium having (a) a large concentration of active sites on the surface of the pores, and (b) a pore size distribution represented by a positively skewed triangular distribution [1] given by

$$\bar{f}(\rho) = \frac{2(\sigma_1 + \rho - 1)}{\sigma_1^2 + \sigma_1 \sigma_2} = \frac{\sigma_1 + \rho - 1}{\sigma_1 \sigma}, \quad 1 - \sigma_1 \le \rho \le 1 \tag{5a}$$

$$\bar{f}(\rho) = \frac{2(\sigma_2 - \rho + 1)}{\sigma_2^2 + \sigma_1 \sigma_2} = \frac{\sigma_2 - \rho + 1}{\sigma_2 \sigma}, \quad 1 \le \rho \le 1 + \sigma_2 \tag{5b}$$

$$\bar{f}(\rho)\, d\rho = f(r)\, dr \tag{5c}$$

$$\int_{r_a}^{r_b} f(r)\, dr = 1 \tag{5d}$$

where

$$\rho = \frac{r}{r_m}, \quad \rho_a = \frac{r_a}{r_m}, \quad \rho_b = \frac{r_b}{r_m} \tag{6}$$

$$\sigma_1 = 1 - \rho_a = 0.25, \quad \sigma_2 = \rho_b - 1 = 0.75 \tag{7}$$

$$2\sigma = \sigma_1 + \sigma_2 = \rho_b - \rho_a = 1.00 \tag{8}$$

In Eqs. (5c), (5d), and (6), r represents the radius of a pore in the pore size distribution $f(r)$, r_a is the radius of the smallest pore in the porous medium, r_b denotes the radius of the largest pore in the porous medium, r_m is the median radius, and $f(r)$ represents

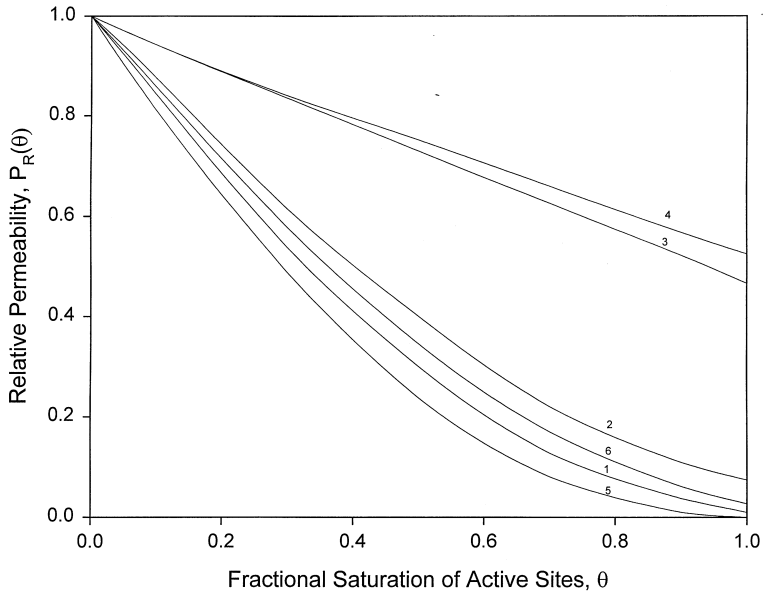

Fig. 1. Relative permeability, $P_R(\theta)$, versus fractional saturation of active sites, θ; Curve 1: $\alpha=0.4$, $\beta=0.0$, $n_T=4$; Curve 2: $\alpha=0.4$, $\beta=0.0$, $n_T=18$; Curve 3: $\alpha=0.2$, $\beta=0.0$, $n_T=4$; Curve 4: $\alpha=0.2$, $\beta=0.0$, $n_T=18$; Curve 5: $\alpha=0.4$, $\beta=0.2$, $n_T=4$; Curve 6: $\alpha=0.4$, $\beta=0.2$, $n_T=18$.

the pore size distribution of the porous medium. The case of $\sigma_1<\sigma_2$ examined here ($\sigma_1=0.25$, $\sigma_2=0.75$) corresponds closely to the pore size distributions determined experimentally by Hagel [3]. The curves in Fig. 1 were generated by fitting the numerical values of $P_R(\theta)$ obtained from the restricted pore diffusion model of Petropoulos et al. [1] which were presented in figure 9 of Ref. [1], with exponential functions of θ that are reported in Reference [4]. The parameters α and β in Fig. 1 represent the dimensionless effective molecular radii of adsorbate A($\alpha=\alpha_1/r_m$ where α_1 is the effective molecular radius of adsorbate A) and ligand (active site), respectively; $\beta=\beta_1/r_m$ where β_1 represents the effective molecular radius of the ligand (active site). The value of the pore connectivity parameter, n_T, in Fig. 1 is varied from 4 to 18 because we want to simulate porous chromatographic media that have both low and high pore connectivities; the value of $n_T=18$ effectively simulates a system of infinite pore connectivity.

The results in Fig. 1 clearly indicate that the macroscopic permeability, P_A, or the macroscopic effective diffusion coefficient, D_A (see Eq. (4)) decreases as (i) the size of the adsorbate and/or ligand (active site) molecule increases, (ii) the fractional saturation, θ, of the active sites increases, and (iii) the pore connectivity, n_T, of the porous network (porous medium) decreases. Furthermore, it is clearly observed in Fig. 1 that for the system represented by curve 5 a percolation threshold ($P_R=0$, $P_A=0$, and $D_A=0$) is attained at $\theta\cong0.96$, and, of course, $P_R=0$, $P_A=0$, and $D_A=0$ for values of $\theta\gtrsim0.96$. The term percolation threshold is used to indicate that at and beyond the value of $\theta\cong0.96$ the adsorbate is effectively excluded from the interior of the porous adsorbent particles, even though a substantial fraction of the pores may be permeable to adsorbate. The exponential functions of θ that were constructed [4] to represent the data in Fig. 1, were employed in the mathematical model of McCoy and Liapis [2] that simulates the dynamic behavior of frontal chromatography in columns packed with porous adsorbent particles, in order to determine the macroscopic effective pore diffusion coefficient, D_A, of adsorbate A at different positions along the particle radius and for particles located at different positions along the axis of the column. The dynamic behavior of frontal chromatography of proteins in columns, was obtained in this work by solving the dynamic model of adsorption of adsorbate A in chromatographic col-

umns developed by McCoy and Liapis [2]. This model [2] accounts for the following mass transfer mechanisms: (a) bulk fluid flow of adsorbate A in the flowing fluid stream of the column, (b) axial dispersion of adsorbate A in the flowing fluid stream of the column, (c) film mass transfer of adsorbate A (mass transfer of adsorbate A through the liquid film surrounding the porous adsorbent particles), (d) diffusion of adsorbate A in the liquid in the pores of the porous adsorbent particles (pore diffusion), and (e) the adsorption mechanism between the molecules of adsorbate A and the active sites on the surface of the pores of the adsorbent particles. In this work, the macroscopic effective pore diffusion coefficient, D_A, that characterizes the mass transfer mechanism of adsorbate A in the porous adsorbent particles (mass transfer mechanism (d)) was determined by the procedure discussed above (for the systems represented by curves 1–6 in Fig. 1), while the adsorption mechanism between the molecules of adsorbate A and the active sites (mass transfer mechanism (e)) was considered to be described by the second-order reversible interaction expression given in Eq. (2). In addition to the macroscopic effective pore diffusion coefficient, D_A, and particle porosity, ε_p, the values of the other parameters used in the column model of McCoy and Liapis [2] to obtain the results in Figs. 2–13 are as follows: $C_{d,in}=0.1$ kg m^{-3}, $C_T=2.2$ kg m^{-3}; $D_L=0$; $K_f=8.93\times10^{-6}$ m s^{-1}; $k_1=2.35\times10^{-2}$ m^3 (kg)$^{-1}$(s)$^{-1}$; $k_2=5.17\times10^{-6}$ s^{-1}; three different column lengths were studied in this work such that the length of the column, L, was taken to be 0.1 m, 0.2 m, and 0.5 m; $R_p=5.0\times10^{-5}$ m; $V_f=3.0\times10^{-4}$ m s^{-1}; $\varepsilon=0.35$; and $\varepsilon_p=0.50$ when $\theta=0$. The value of the axial dispersion coefficient, D_L, was taken to be zero because the estimated value of D_L from expressions presented in Heeter and Liapis [5] is so low that the error introduced, by setting D_L equal to zero in the model of McCoy and Liapis [2], in the calculated dynamic behavior of the column systems [5] is insignificant.

3. Results and discussion

In Figs. 2–4, the breakthrough curves for the adsorption systems represented by curves 1–6 in Fig. 1 are presented for column lengths of 0.1 m, 0.2 m, and 0.5 m. The results clearly show that the time at which breakthrough occurs decreases as the magnitude of the macroscopic effective pore diffusion

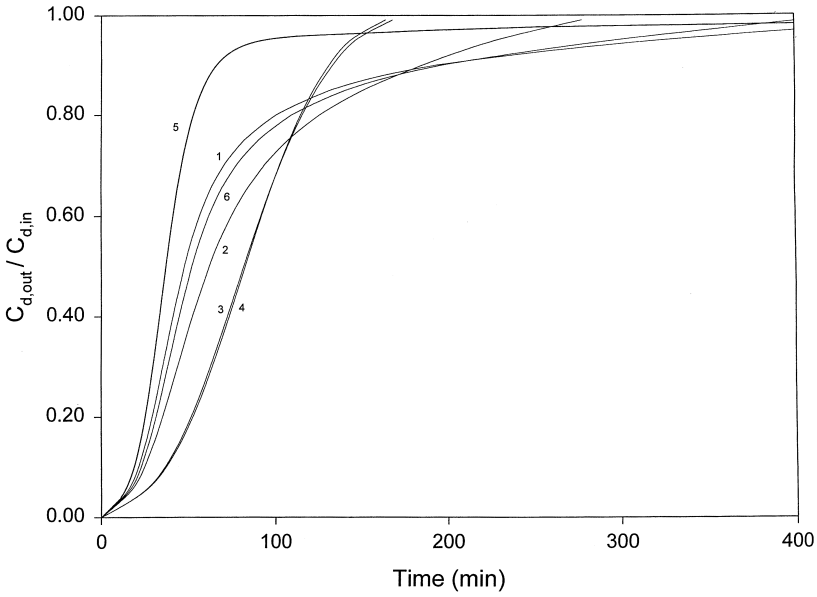

Fig. 2. Breakthrough curves for the adsorption systems represented by curves 1–6 in Fig. 1 when the column length L is 0.1 m.

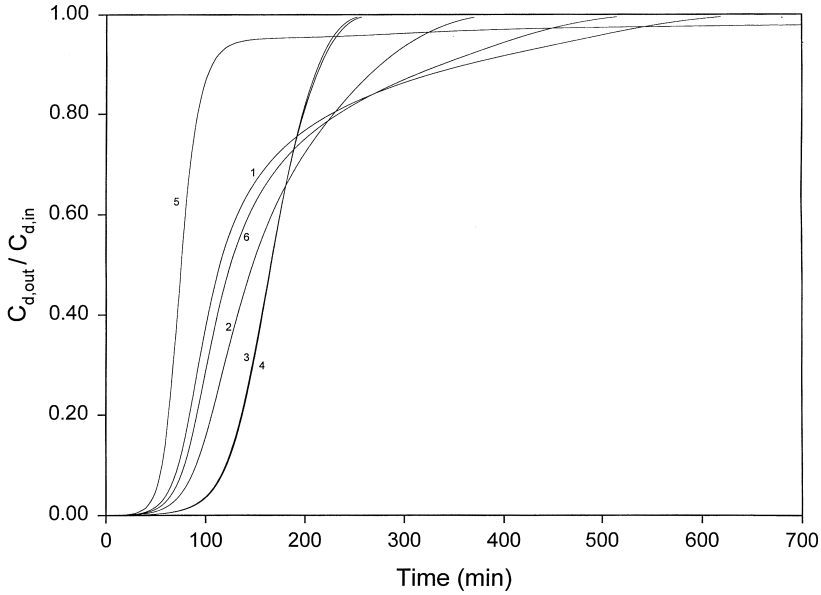

Fig. 3. Breakthrough curves for the adsorption systems represented by curves 1–6 in Fig. 1 when the column length L is 0.2 m.

coefficient D_A (or macroscopic permeability P_A) of the adsorbate A in the adsorbent particles decreases. It can also be observed that the breakthrough curves of the adsorption systems represented by curves 1–6 in Fig. 1, follow the trend established by the results in Fig. 1 with respect to the effects of the values of α, β, and n_T. Furthermore, the results in Figs. 2–4 indicate that as the column length L increases (and

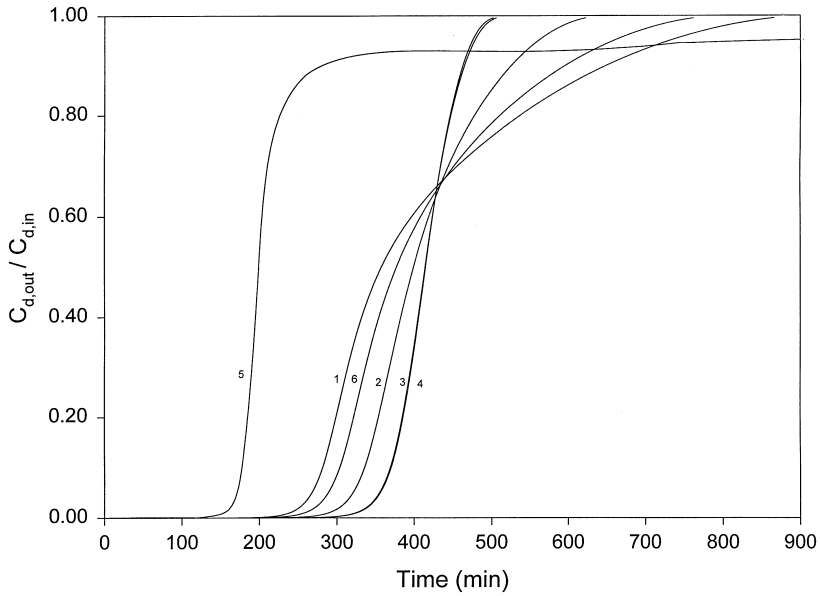

Fig. 4. Breakthrough curves for the adsorption systems represented by curves 1–6 in Fig. 1 when the column length L is 0.5 m.

thus, the residence time of the adsorbate molecules in the column increases) the time at which breakthrough occurs increases significantly for each adsorption system represented by the curves 1–6 in Fig. 1, and the increase in breakthrough time is substantially larger for the adsorption systems whose macroscopic effective pore diffusion coefficient, D_A, is higher for a given value of the fractional saturation of the active sites, θ. This occurs because as the residence time of the adsorbate molecules increases with increasing column length, there is more time available for the development of larger mean concentration gradients in the pore fluid of the adsorbent particles which lead to larger mean mass fluxes of adsorbate A in the adsorbent particles; these larger mean mass fluxes result in larger amounts of adsorbate A being in the adsorbed phase.

The results in Figs. 5–7 present the total amount of mass of adsorbate A in the adsorbed phase of a column of length 0.1 m, 0.2 m, and 0.5 m, respectively, as a function of percent breakthrough, for the adsorption systems represented by curves 1–6 in Fig. 1. The results clearly show that the effect of percent breakthrough, for a given adsorption system (the different adsorption systems are represented by curves 1–6), on the total amount of mass of adsorbate A in the adsorbed phase of the column decreases as the column length increases. This is due to the fact that, as discussed above, the increased residence times of the adsorbate molecules with increasing column length, L, lead to larger mean mass fluxes of adsorbate A in the adsorbent particles which in turn result in larger amounts of adsorbate A in the adsorbed phase for a given percent breakthrough, and this leads to a weakening of the effect of the percent breakthrough on the total mass of adsorbate adsorbed as the column length increases. Furthermore, the results in Figs. 5–7 follow the trend established by the data in Fig. 1 with respect to the effects of the values of α, β, and n_T.

In Figs. 8–13 the dimensionless average concentration $\bar{C}'_s$, versus the dimensionless position, x/L, along the column is presented for 5% and 10% breakthrough, when the length of the column, L, is 0.1 m, 0.2 m, and 0.5 m. The variable $\bar{C}'_s$ is given by

$$\bar{C}'_s = \frac{\bar{C}_s}{C_T} \tag{9}$$

where

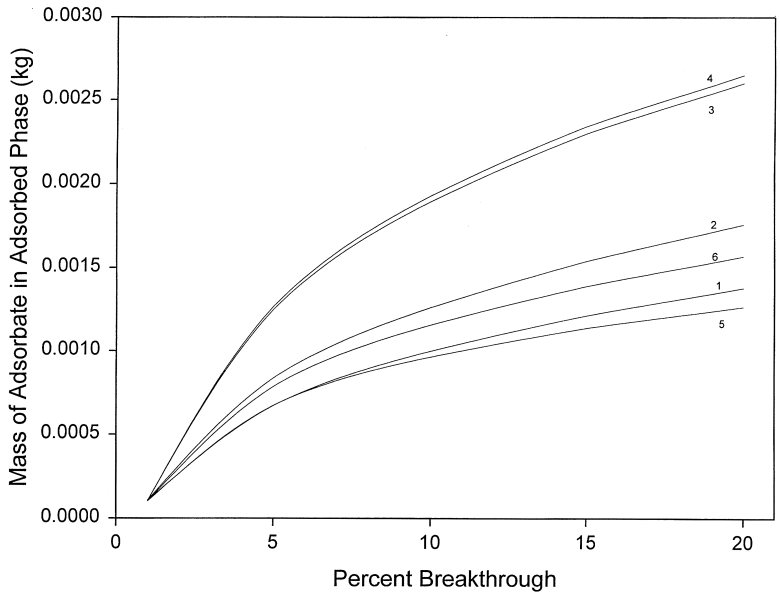

Fig. 5. Total amount of adsorbate in the adsorbed phase at different values of percent breakthrough, for the adsorption systems represented by curves 1–6 in Fig. 1 when the column length L is 0.1 m.

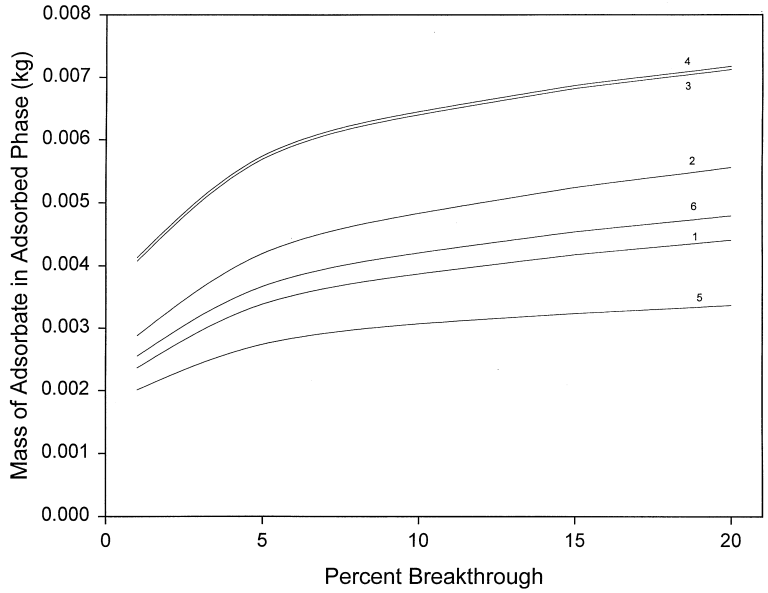

Fig. 6. Total amount of adsorbate in the adsorbed phase at different values of percent breakthrough, for the adsorption systems represented by curves 1–6 in Fig. 1 when the column length L is 0.2 m.

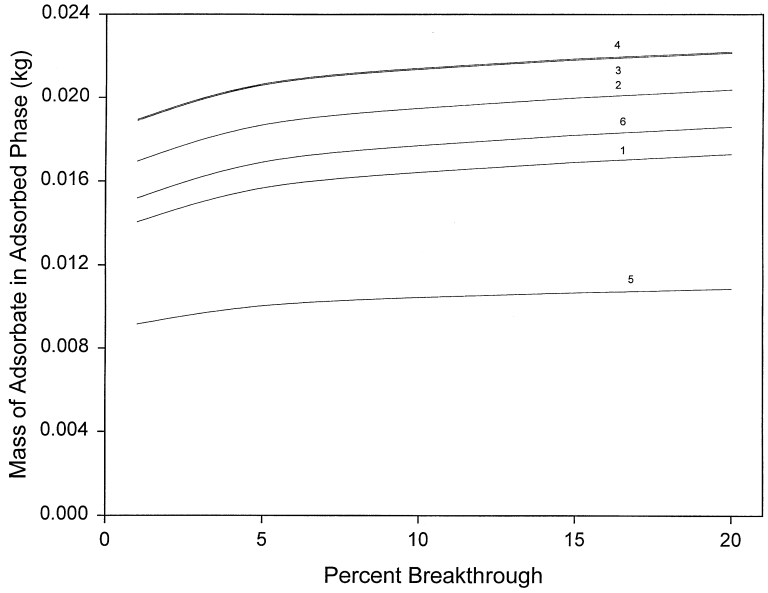

Fig. 7. Total amount of adsorbate in the adsorbed phase at different values of percent breakthrough, for the adsorption systems represented by curves 1–6 in Fig. 1 when the column length L is 0.5 m.

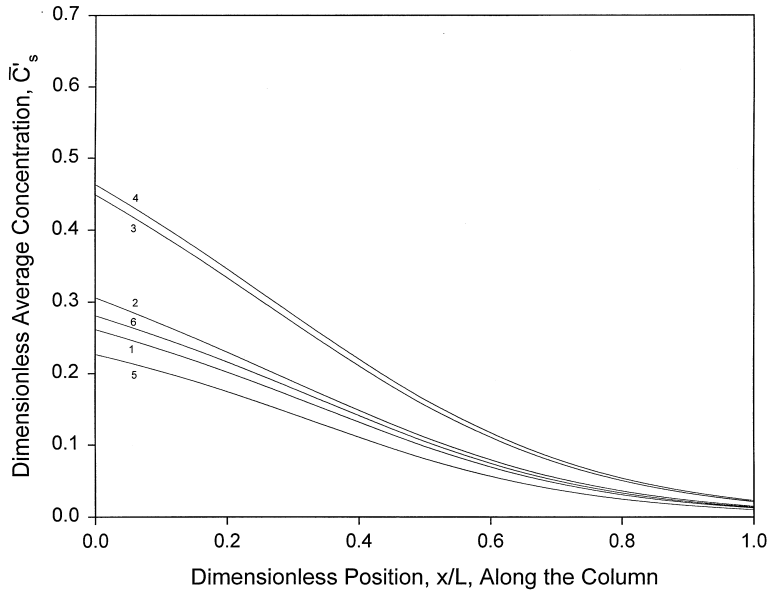

Fig. 8. Dimensionless average concentration of adsorbate in the adsorbed phase, $\bar{C}'_s$, at 5% breakthrough as a function of the dimensionless position x/L along the column, for the adsorption systems represented by curves 1–6 in Fig. 1 when the column length L is 0.1 m.

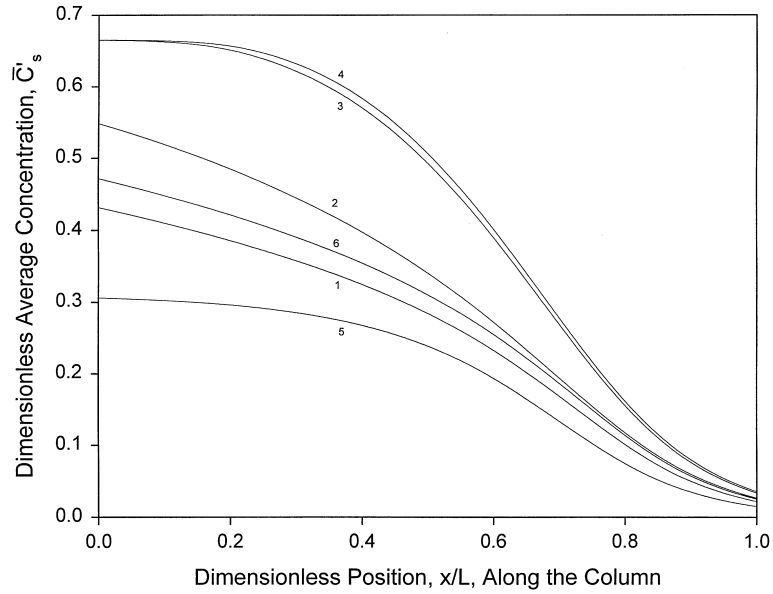

Fig. 9. Dimensionless average concentration of adsorbate in the adsorbed phase, $\bar{C}'_s$, at 5% breakthrough as a function of the dimensionless position x/L along the column, for the adsorption systems represented by curves 1–6 in Fig. 1 when the column length L is 0.2 m

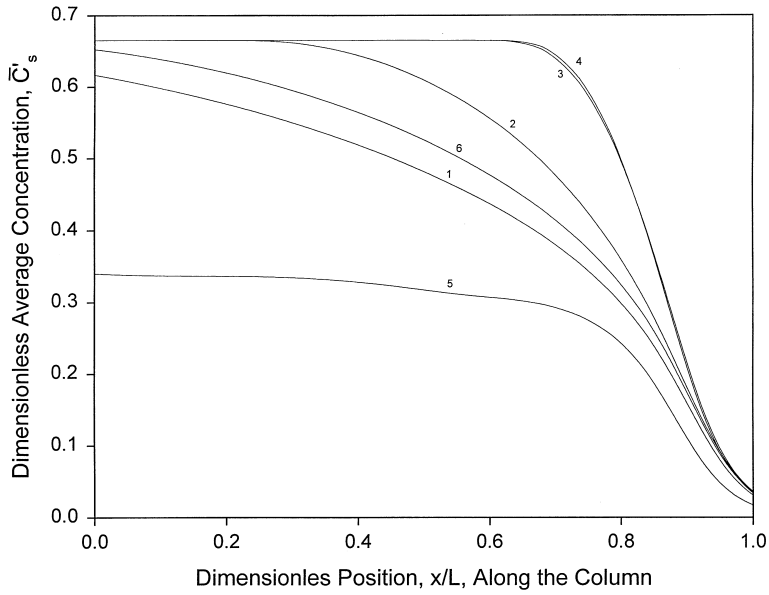

Fig. 10. Dimensionless average concentration of adsorbate in the adsorbed phase, $\bar{C}'_s$, at 5% breakthrough as a function of the dimensionless position x/L along the column, for the adsorption systems represented by curves 1–6 in Fig. 1 when the column length L is 0.5 m.

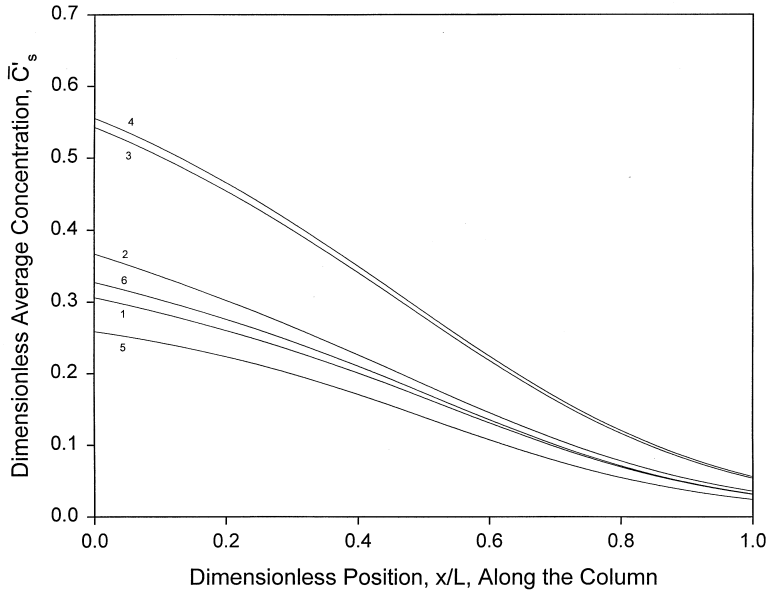

Fig. 11. Dimensionless average concentration of adsorbate in the adsorbed phase, $\bar{C}'_s$, at 10% breakthrough as a function of the dimensionless position x/L along the column, for the adsorption systems represented by curves 1–6 in Fig. 1 when the column length L is 0.1 m.

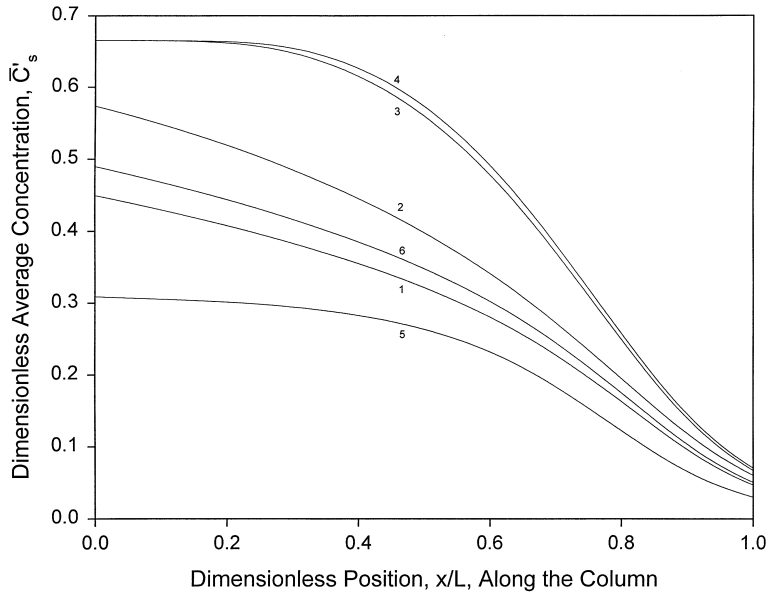

Fig. 12. Dimensionless average concentration of adsorbate in the adsorbed phase, $\bar{C}'_s$, at 10% breakthrough as a function of the dimensionless position x/L along the column, for the adsorption systems represented by curves 1–6 in Fig. 1 when the column length L is 0.2 m.

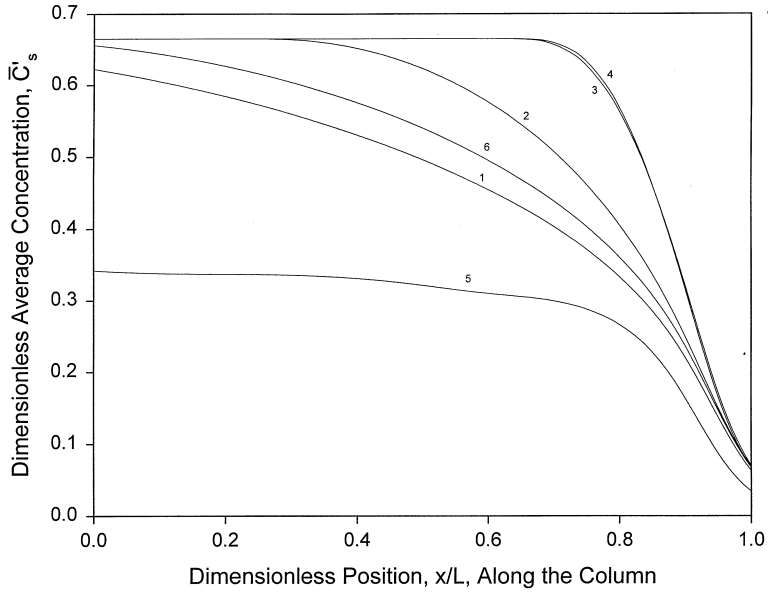

Fig. 13. Dimensionless average concentration of adsorbate in the adsorbed phase, $\bar{C}'_s$, at 10% breakthrough as a function of the dimensionless position x/L along the column, for the adsorption systems represented by curves 1–6 in Fig. 1 when the column length L is 0.5 m.

$$\bar{C}_s = \frac{3}{R_p^3} \int_0^{R_p} C_s R^2 \, dR \qquad (10)$$

The results in Figs. 8–13 clearly show that, for every adsorption system represented by curves 1–6, the adsorptive capacity of the chromatographic particles, considering that the inlet concentration, $C_{d,in}$, of adsorbate A is equal to 0.1 kg m^{-3}, is more efficiently used at each position x/L along the column as the column length L and the percent breakthrough are increased. The effect of increasing the column length in order to utilize the adsorptive capacity of the particles more efficiently is significantly more important than the effect of increasing the percent breakthrough. Thus, the data in Figs. 8–13 indicate that, for chromatographic systems with restricted pore diffusion, the adsorptive capacity of the chromatographic particles can be used more efficiently at each position along the column by increasing the length L of the column. Also, the results in Figs. 8–13 follow the trend indicated by the data in Fig. 1 with respect to the effect of the values of α, β, and n_T.

4. Conclusions and remarks

In this work, a theoretical formulation was presented that can be used to describe the dynamic behavior of frontal chromatography of proteins in columns packed with adsorbent particles in which restricted pore diffusion of the adsorbate molecules occurs. The results of this work clearly show that the time for breakthrough and the effective utilization of the adsorptive capacity of the chromatographic particles increase as (a) the size of the adsorbate and/or ligand (active site) molecule decreases, (b) the pore connectivity, n_T, of the porous network of the adsorbent particles increases, and (c) the column length, L, increases. Therefore, for the chromatographic separation of an adsorbate of interest, the deleterious effects of restricted pore diffusion can be significantly reduced if (i) the adsorbent particles have high pore connectivity, n_T, (ii) the ligand (active site) molecules immobilized on the surface of the pores of the adsorbent particles are of small size, and (iii) the chromatographic columns, in which the adsorbent particles are to be packed, are not short.

5. Notation

A	Adsorbate
$C_{d,in}$	Concentration of adsorbate A at the column inlet, kg m^{-3} of bulk fluid
$C_{d,out}$	Concentration of adsorbate A at the column outlet, kg m^{-3} of bulk fluid
C_p	Concentration of adsorbate A in the fluid of the pores of the adsorbent particle, kg m^{-3} of pore fluid
C_s	Concentration of adsorbate A in the adsorbed phase of the adsorbent particle, kg m^{-3} of adsorbent particle
$\bar{C}_s$	Average concentration of adsorbate A in the adsorbed phase of the adsorbent particle given by Eq. (10), kg m^{-3} of adsorbent particle
$\bar{C}'_s$	Dimensionless average concentration of adsorbate A in the adsorbed phase of the adsorbent particle ($\bar{C}'_s = C_s/C_T$)
C_T	Maximum equilibrium concentration of adsorbate A in the adsorbed phase of the adsorbent particle, kg m^{-3} of adsorbent particle
D_A	Macroscopic effective pore diffusion coefficient of adsorbate A in the porous adsorbent particle, m^2 s^{-1}
D_L	Axial dispersion coefficient of adsorbate A, m^2 s^{-1}
$f(r)$	pore size distribution
$f(\rho)$	pore size distribution
k_1	Rate constant in Eq. (1) and Eq. (2), m^3 kg^{-1} s^{-1}
k_2	Rate constant in Eq. (1) and Eq. (2), s^{-1}
K	Equilibrium constant ($K = k_1/k_2$), m^3 kg^{-1}
K_f	Film mass transfer coefficient of adsorbate A, m s^{-1}
L	Length of column, m
n_T	Pore connectivity, dimensionless
P_A	Macroscopic permeability of adsorbate A in the porous adsorbent particle, m^2 s^{-1}

$P_R(\theta)$ Relative permeability of adsorbate A in the porous adsorbent particle (defined in Eq. (3)), dimensionless
r Radius of a pore in the pore size distribution of the porous adsorbent particle, m
r_a Radius of smallest pore in the pore size distribution of the porous adsorbent particle, m
r_b Radius of largest pore in the pore size distribution of the porous adsorbent particle, m
r_m Median radius, m
R Radial distance in adsorbent particle, m
R_p Radius of adsorbent particle, m
t Time, s
V_f Superficial fluid velocity, m s^{-1}
x Axial distance in column, m

Greek characters

α Dimensionless effective molecular radius of adsorbate A ($\alpha = \alpha_1 / r_m$)
α_1 Effective molecular radius of adsorbate A, m
β Dimensionless effective molecular radius of ligand ($\beta = \beta_1 / r_m$)
β_1 Effective molecular radius of ligand, m
ε Void fraction in column
ε_p Porosity of the porous adsorbent particle
θ Fractional saturation of ligands (active sites)
ρ Normalized pore radius ($\rho = r / r_m$)
σ Reduced width of the pore size distribution (Eq. (8))
σ_1, σ_2 Reduced widths associated with the positively skewed triangular pore size distribution

Acknowledgement

The authors gratefully acknowledge partial support of this work by Monsanto.

References

[1] J.H. Petropoulos, A.I. Liapis, N.P. Kolliopoulos, J.K. Petrou, N.K. Kanellopoulos, Bioseparation 1 (1990) 69.
[2] M.A. McCoy, A.I. Liapis, J. Chromatogr. 548 (1991) 25.
[3] L. Hagel, in: P. Dubin (Ed.) Aqueous Size Exclusion Chromatography, Elsevier, Amsterdam, The Netherlands, 1988, pp. 1–37.
[4] O. K. Crosser, Internal Report Number 11, Department of Chemical Engineering, University of Missouri-Rolla, Rolla, Missouri, USA, 1998.
[5] G.A. Heeter, A.I. Liapis, J. Chromatogr. A 796 (1998) 157.